技術論文

Development of Strength Analysis Method for Off-Road Motorcycle Radiator Assembly

Masakazu Yamaya　Akihiro Chiba

当論文は、SAE 2013-32-9043 / JSAE 20139043として、台北(台湾)にて行われたSETC2013(Small Engine Technology Conference)で発表されたものです。

DOI: 10.4271/2013-32-9043

要旨

水冷エンジンを搭載したオフロードモーターサイクルのラジエータは、一般的に車体側面に取り付けられている。そのため、モーターサイクルが転倒するとラジエータは樹脂外装を介して地面とぶつかり衝撃を受ける。そして、ラジエータは変形し、冷却性能の低下や冷却水の漏れに至ることがある。当社では、低速走行で転倒した時にラジエータが容易に変形しないように、ラジエータ本体とラジエータを覆う樹脂外装の強度設計を行っている。しかし、強度試験におけるラジエータの挙動は複雑なので、実験だけで強度対策をすると試行錯誤が必要となる。そこで、強度設計を支援するためのシミュレーション手法を開発した。

Abstract

The radiator assembly for a liquid-cooled off-road motorcycle is generally attached to the side of the frame. Therefore, if the motorcycle topples over, the radiator may strike the ground and receive an impact through the plastic side cover. This may deform the radiator, reducing its cooling performance or leading to a coolant leak. The strength of the radiator and plastic side cover was designed so that the radiator assembly will not deform easily if the motorcycle topples over at low speeds. However, due to the complex behavior of the radiator assembly in strength tests, a degree of trial-and-error may be necessary to incorporate strength countermeasures by tests alone. Therefore, a strength test simulation method was developed to help design the required strength of radiator assemblies.

1 INTRODUCTION

The radiator for a liquid-cooled off-road motorcycle is generally attached to the side of the frame and covered with a plastic cover. As a result, if the motorcycle topples over, the radiator and plastic cover may strike the ground and receive an impact. This may deform the radiator, reducing its cooling performance or leading to a coolant leak.

Strength was designed so that the radiator will not deform easily if the motorcycle topples over when traveling at extremely low speeds. However, the behavior of the breakage process for the radiator and plastic cover is complex, and it is difficult to identify the exact locations for strength countermeasures and to estimate the reinforcement effects. As a result, testing of strength countermeasures by vehicle tests alone may require large numbers of prototype parts and large amounts of time. Therefore, a strength test simulation method was developed to help design the required strength of radiator and plastic cover.

For this study, strength tests were conducted of the plastic cover and radiator individually, and of the radiator assembly when these components are assembled together. The validity of the simulation models for the plastic cover and radiator individually, and for the radiator assembly, was verified based on the results from these tests, and the results demonstrated the effectiveness of this simulation method.

2 STRENGTH TESTS OF THE RADIATOR ASSEMBLY AND INDIVIDUAL COMPONENTS

To verify the suitability of this simulation method, three types of bench tests were performed using the individual plastic cover, the individual radiator, and a radiator assembly combining the plastic cover and radiator. Guidelines for construction of a simulation method were obtained during the course of these tests. Strength tests were performed using the radiator and plastic cover of off-road motorcycle with a liquid-cooled 250 cc engine. The appearance of the radiator and plastic cover is shown in Figure 1.

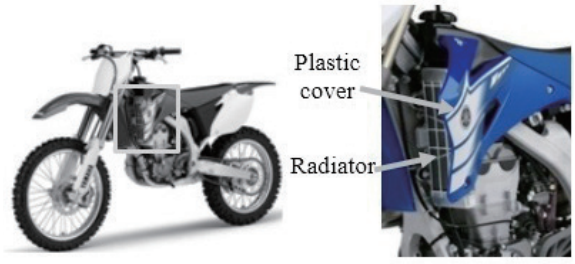

Figure 1: Appearance of radiator and plastic cover

3 RADIATOR ASSEMBLY STRENGTH TEST

The bench tests have been performed to design the required strength of the radiator and the plastic cover, because tests which involve actually toppling the vehicle suffer from poor reproducibility, and the evaluation is difficult. The focus of the tests was damage to the radiator and plastic cover caused when the motorcycle topples over while traveling at extremely low speed. Figure 2 shows the conditions of damage to the radiator and plastic cover caused when the motorcycle toppled over at extremely low speed. Because contact with the ground was via the plastic cover, the fins and core support were damaged and buckling of the plastic cover occurred.

The bench tests evaluated the maximum reaction force of the radiator assembly as a substitute characteristic for strength design in case the motorcycle topples over. This test method focused on reproducing the damage conditions of the radiator and plastic cover when the motorcycle toppled over, and identifying the locations to take strength countermeasures. For this reason, the test speed was not set based on the impact that occurs when the motorcycle topples over. The criteria for maximum reaction force are now being studied. The results from previous tests have made it clear that coolant leakage will not occur when the maximum reaction force is at or above a particular value.

The appearance of radiator assembly strength test is shown in Figure 3. The radiator and plastic cover were assembled onto a frame which is fastened in 1G' conditions (empty vehicle standing vertical). The radiator was bolted to the frame via a grommet. The plastic cover was bolted to a bracket installed on the radiator side and to the fuel tank and to the frame. The impact load when the motorcycle topples over was estimated based on the conditions of resulting damage to the radiator and side cover, and were used as a static load at the bench test. For the bottom end of the radiator, which is the part most likely to contact the ground when the motorcycle topples over, the load is applied in the direction of the vehicle rear.

The conditions of the radiator and plastic cover after reproducing the damage conditions by means of bench test are shown in Figure 4. The bench test succeeded in reproducing the conditions of damage to the radiator and the buckling of the plastic cover which occur when the motorcycle topples over.

To verify the suitability of this simulation method, the test was performed with two models of radiator assembly: Model A and Model B. The primary difference between the two models is the thickness of the side cover. Model A is approximately 10% thicker than Model B. The appearance is shown in Figure 5. A portable fatigue tester (KYB, KPL-5kN) was used to apply load in the direction from the front of the vehicle. The pushing speed was 500 mm/min. The load cell and displacement gauge built into the tester were used to measure the displacement of the push jig towards the rear of the vehicle and the reaction force generated by the radiator assembly.

The created load-displacement curve is shown in Figure 6. The plastic cover began to buckle when pushed by approximately 20% of the specified stroke (Point a,

Figure 6). The differences in the maximum reaction force among different vehicle models were virtually identical to the differences in reaction force at the time when the plastic cover began to buckle. Therefore, it is necessary to reproduce the buckling of the plastic cover in order to accurately find the maximum reaction force of the radiator assembly.

After the test, dents were found in the radiator components that are thought to have been caused by interference with surrounding parts. In order to reproduce the damage to the radiator caused by this interference, it was decided to create a model of the frame and other parts which surround the radiator.

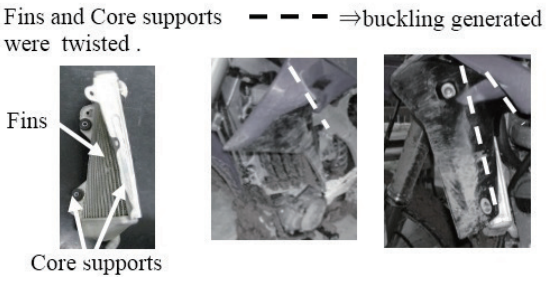

Figure 2: Damage conditions of radiator and plastic cover

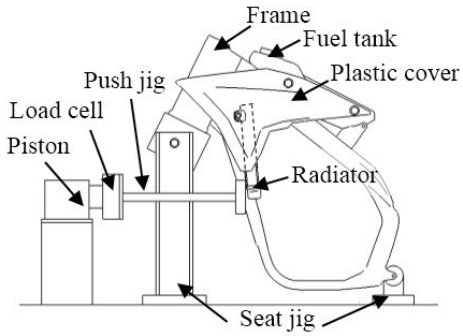

Figure 3: Appearance of radiator assembly strength test

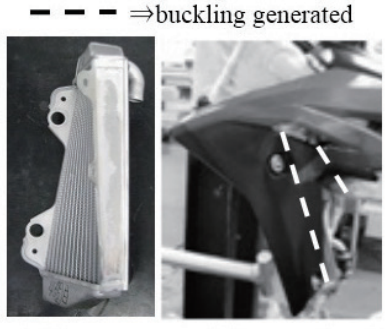

Figure 4: Damage conditions of radiator and plastic cover

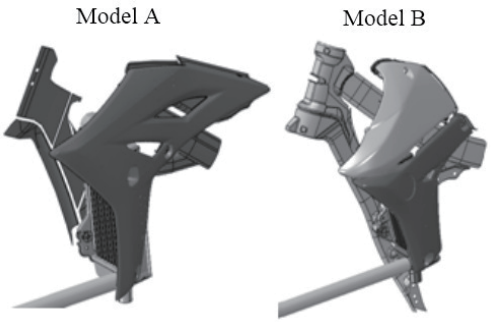

Figure 5: Appearance of radiator assembly model A and B

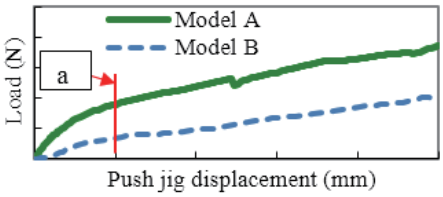

Figure 6: Results of radiator assembly strength test

4 PLASTIC COVER INDIVIDUAL COMPONENTS STRENGH TEST

A compression test of the plastic cover was conducted using a universal tester (Shimazu, Autograph, AG-25TA). The test conditions are shown in Figure 7. The load cell and displacement gauge built into the tester were used to measure the reaction force of the plastic cover and the displacement of the push jig in the direction perpendicular to the surface plate. A fuel tank filled with mortar to ensure rigidity was installed as the support onto the seat jig, and the plastic cover was installed onto the tank. Some of the bolt fastening points for the plastic cover are located on the fuel tank.

For the radiator assembly strength test, a push jig was used to apply a load to the radiator, and this load was transmitted via the radiator to the plastic cover. For the plastic cover individual component test, in order to reproduce the load transmission that occurs during the assembly test, a push jig which applies the load was installed onto the position where the plastic cover is mounted onto the radiator. In order to determine the effects of plastic strain rate sensitivity, three pushing speeds were set (10 mm/min, 100 mm/min, and 500

mm/min), and the test temperature was set to room temperature.

The load-displacement curve that was created from the test results is shown in Figure 8. The reason that the load decreases when approximately 20% of the specified stroke is reached is that the plastic cover buckles as shown in Figure 9. These load-displacement curves show that the maximum load (buckling load) changes at different speeds even within the range of the pushing speeds that are assumed in the assembly strength test, indicating rate sensitivity. Based on these result, it was decided to consider strain rate sensitivity in the plastic cover model.

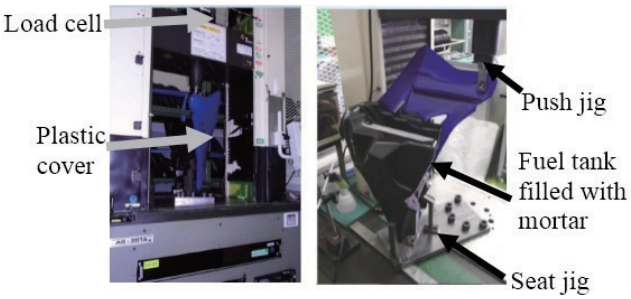

Figure 7: Plastic cover individual component strength test

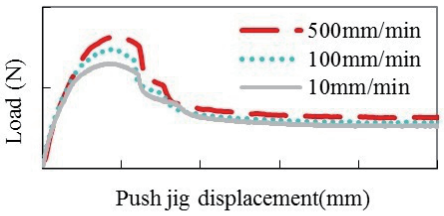

Figure 8: Results of plastic cover individual component strength test

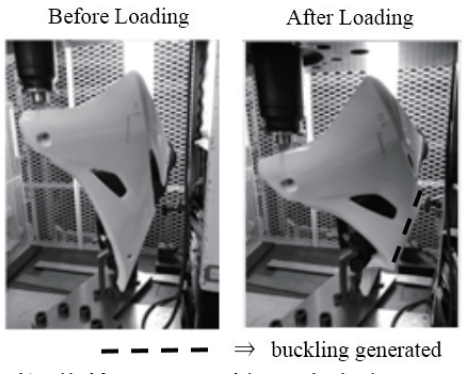

Figure 9: Damage condition of plastic cover

5 RADIATOR INDIVIDUAL COMPONENT STRENGTH TEST

A compression test of the radiator was conducted using a universal tester (Shimazu, Autograph, AG-25TA). The test conditions are shown in Figure 10. In order to decide whether or not it was necessary to model the heat-radiating fins, strength tests were performed for an ordinary radiator and a radiator with the fins cut off. The appearance of the radiator without the fins is shown in Figure 11.

The load cell and displacement gauge built into the tester were used to measure the reaction force of the radiator and the displacement of the push jig in the direction perpendicular to the surface plate. The load point was the point that is expected to contact the ground when the motorcycle topples over. The pushing speed was 10 mm/min.

The load-displacement characteristics were created from the test results as shown in Figure 12. This load-displacement curve shows that the reaction force generated by the fins accounts for approximately 50% of the reaction force generated by the radiator. Although the thickness of each fin is only approximately 0.1 mm, it is believed that the fins have a large effect on the radiator reaction force due to the large number of fins. Based on these results, it was decided not to omit the fins when creating the model.

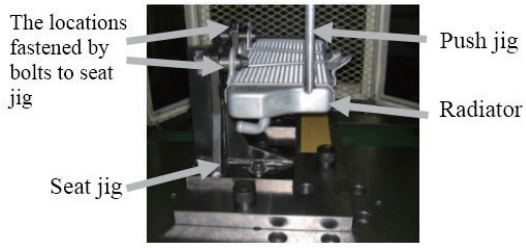

Figure 10: Radiator individual component strength test

Figure 11: Radiator without fins

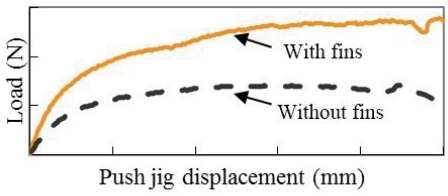

Figure 12: Results of radiator individual component strength test

6 STRENGTH SIMULATIONS OF THE RADIATOR ASSEMBLY AND INDIVIDUAL COMPONENTS

Simulations of the plastic cover individual component test and the radiator individual component test were performed and compared with the test results. The methods used to construct the simulation models of the radiator and plastic cover were used to simulate the radiator assembly strength for two vehicle models. The strength analysis code is the Abaqus.

7 PLASTIC COVER INDIVIDUAL COMPONENTS STRENGTH SIMULATION

The simulation model is shown in Figure 13. A dynamic explicit analysis method was used to produce a stable buckling solution. The model of the plastic cover was created using shell elements. Meshing with element dimensions of approximately 5 mm was performed at the rib sheet center, and for all other parts at the sheet exterior.

The plastic cover was installed onto the fuel tank, and fastened to the fuel tank which was expressed as a rigid body. The fuel tank reference node was fixed. The locations fastened by bolts were expressed by multipoint constraint, and constraint around the bolt center axis was free. The plastic cover and the fuel tank can interact with each other by contact definition. Multiple points around the mounting point of the push jig were constrained in order to forcibly vary the position of the reference node. The load was applied to the reference node in the X-axis direction. The pushing speed was 500 mm/min.

The stress-strain characteristics included consideration of strain rate sensitivity. The strain rate sensitivity was determined by tensile tests performed at room temperature. The test pieces shapes were JIS No. 2 shapes, and the test pieces were made of the same material as the plastic cover. The results of the true stress-strain characteristics that were found based on the measurement results are shown in Figure 14. Because the strain speed of 100 (1/sec) produced significant noise due to impact, it was decided to treat the plastic cover as an elastic-perfectly plastic solid at strain speed of 100 and to generate constant stress equivalent to the tensile strength.

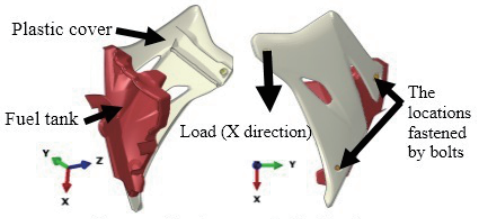

Figure 13: Plastic cover individual component strength test model

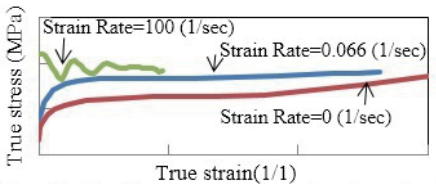

Figure 14: Plastic cover stress-strain characteristics

8 VERIFICATION OF PLASTIC COVER INDIVIDUAL COMPONENT STRENGTH SIMULATION

The conditions of total internal energy and total kinetic energy generation for all elements of the plastic cover model are shown in Figure 15. The percentage of total kinetic energy relative to internal energy is on the order of several percent, showing that a valid solution can be provided by addressing the issue as a quasi-static problem.

Figure 16 shows the load-displacement curve that was created from the simulation results. The load and displacement in the simulation results represent the reaction force and displacement of the load point in the X direction. The maximum load is approximately 10% higher in the simulation result than the test result. The reason is believed to be the higher rigidity resulting from thickness that is larger in the model than in the actual plastic cover at locations such as where the thickness changes gradually. The damage conditions from the simulation are shown in Figure 17. The Figure shows how the conditions of plastic cover buckling were reproduced.

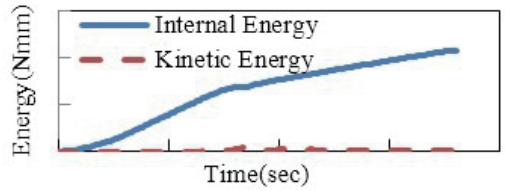

Figure 15: Energy in plastic cover model

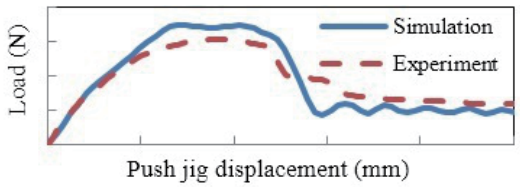

Figure 16: Plastic cover load-displacement curve

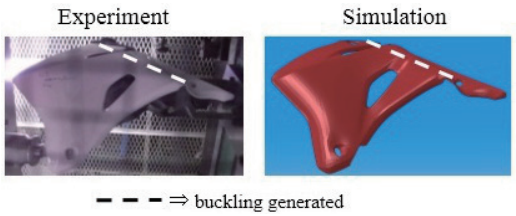

Figure 17: Conditions of plastic cover deformation

9 RADIATOR INDIVIDUAL COMPONENT STRENGTH SIMULATION

The simulation model is shown in Figure 18. A dynamic explicit analysis method was used to provide a final solution in combination with the plastic cover.

The push jig and seat jig were considered to be rigid bodies, and only the parts of the seat jig which may contact the radiator were modeled. The radiator is a brazed thin-walled aluminum part. The brazing in the simulation model was expressed using multi-point constraints. All parts other than the heat-radiating fins were modeled using shell elements. Meshing with element dimensions of approximately 3～5mm was performed. The radiator was fastened to the seat jig which was expressed as a rigid body. The seat jig reference node was fixed. The locations fastened by bolts were expressed by multipoint constraint, and constraint around the bolt center axis was free. The radiator and the seat jig, the radiator and the push jig can interact with each other by contact definitions. The load was applied to the bottom end of the radiator in the Y-axis direction via a push jig. The stress-strain characteristics for the water tank and core support were found from tensile tests performed using test pieces that were cut from the product. The stress-strain characteristics are shown in Figure 19. Locations where it was difficult to cut out a sample were estimated based on the results from hardness measurement.

For the fins, faithfully creating the actual fin shapes and fitting them into the radiator model would require much time and is not a good method for operating a simulation. Therefore, the fins were created using a user material (dynamic stress-strain relation in the Abaqus) for honeycombs in order to create a material model with equivalent mechanical behaviors to the fins, and the model was created using solid elements (hereinafter referred to as the "simulated fin model").

The simulated fin model is shown in Figure 20 and 21. The parameters for the user materials were decided from calibration. Calibration was determined by adjustment so that the load-displacement responses of the fin unit model and simulated fin model were the same. The fin unit model is shown in Figure 20 and 21. This is a model of a block shape approximately 5 mm x 7 mm in size that was cut out of a continuous heat-radiating fin to serve as one unit. It simulates the load via rigid sheets in the X-axis and Y-axis directions shown in Figure 21. The load-displacement curves created based on the calculation results from the fin unit model and simulated fin model are shown in Figure 22. The load and displacement in the simulation results represent the reaction force and displacement of the reference node of the rigid seat in the Y direction. The response of the fin unit model was reproduced by the simulated fin model.

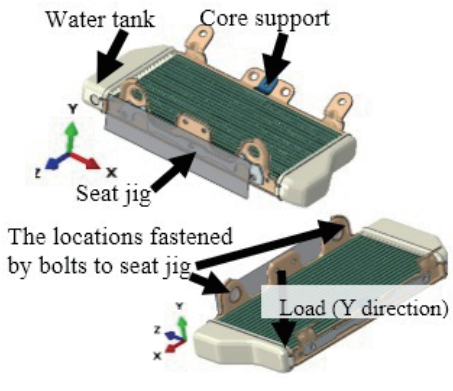

Figure 18: Radiator individual component strength test model

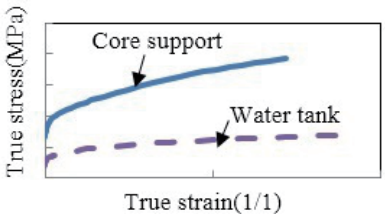

Figure 19: Radiator stress-strain characteristics

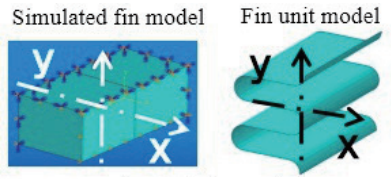

Figure 20: Fin models

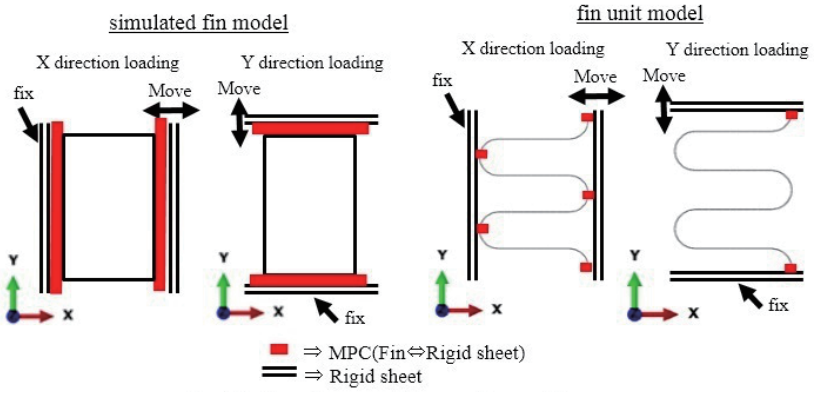

Figure 21: Boundary conditions of fin models

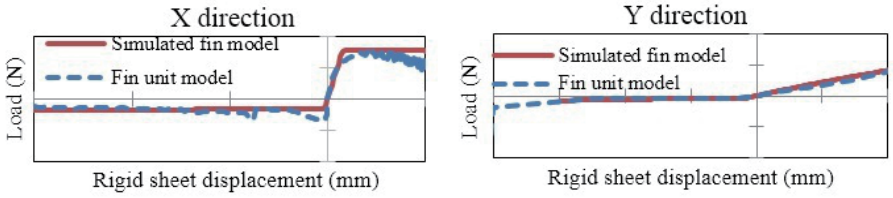

Figure 22: Fin model load-displacement curves

10 VERIFICATION OF RADIATOR INDIVIDUAL COMPONENT STRENGTH SIMULATION

Figure 23 shows the conditions of total internal energy and total kinetic energy generation for all elements of the radiator model. The percentage of total kinetic energy relative to internal energy is on the order of several percent, showing that a valid solution can be provided by addressing the issue as a quasi-static problem.

Figure 24 shows the load-displacement curves that were created from the simulation results. The load and displacement in the simulation results represent the reaction force acting on the push jig in the Y-axis directions, and the displacement of the push jig in the Y-axis directions. The generated load is approximately 20% higher in the radiator model on which heat radiating fins are reproduced than in the test. The reason is believed to be that the rigidity of the fin unit model is higher than the actual fins because the model omits the slits that are machined on the surface of the actual fins, resulting in the higher rigidity of the simulated fin model than the actual fins. Figure 25 shows the conditions of deformation in the radiator model with fins after the load was removed. The damage conditions from the test, in which the radiator became twisted, were reproduced.

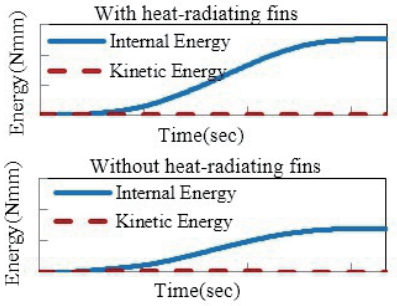

Figure 23: Energy in radiator model

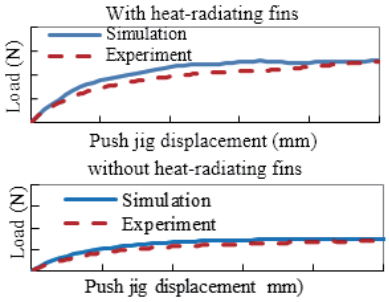

Figure 24: Radiator model load-displacement curves

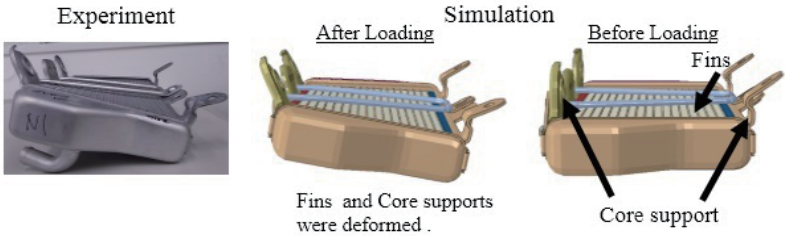

Figure 25: Conditions of radiator model deformation

11 RADIATOR ASSEMBLY STRENGTH SIMULATION

The methods used to construct the simulation models of the radiator and plastic cover were used to simulate the radiator assembly strength for two vehicle models. The simulation models are shown in Figure 5 and 26.

In order to reproduce the damage caused to the radiator by interference with surrounding parts (such as frame, fuel tank), Rigid bodies were used to create models of these surrounding parts. These rigid bodies reference nodes were fixed. All parts can interact with each other by contact definitions. The locations fastened by bolts were expressed by multipoint constraint, and constraint around the bolt center axis was free. The radiator was bolted to the frame via a grommet. The load was applied to the bottom end of the radiator in the X-axis direction via a push jig. The pushing speed was 500 mm/min.

A rigidity simulation of the grommet individual component was performed in advance, and the resulting load-displacement response was incorporated as a non-linear spring element to simulate the behavior of the grommet. The rigidity simulation model for the grommet individual component is shown in Figure 27. The grommet is a hyperelastic body and the strain energy potential function is a Yeoh type. The seat jig and the push jig are rigid body. The seat jig reference node was fixed. The grommet and the seat jig, the grommet and the push jig can interact with each other by contact definitions. The load was applied to the three axis directions and around the X and Z-axes via a push jig.

The rigidity calculation results are shown in Figure 28. The load and displacement in the simulation results represent the reaction force acting on the push jig in the three axis directions, and the displacement of the push jig in the three axis directions. The torque and rotation angle represent the torque acting on the push jig around the X and Z axes, and the rotation of the push jig around the X and Z axes.

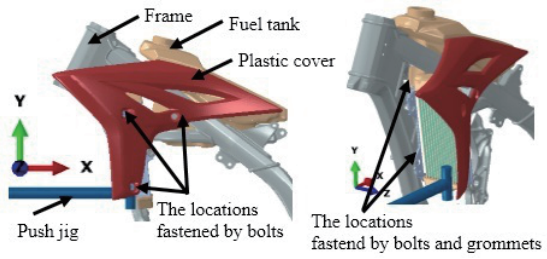

Figure 26: Radiator assembly strength simulation model

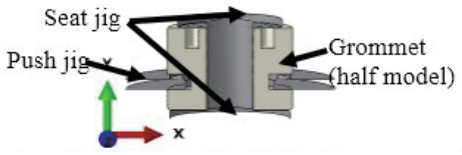

Figure 27: Grommet individual component rigidity simulation model

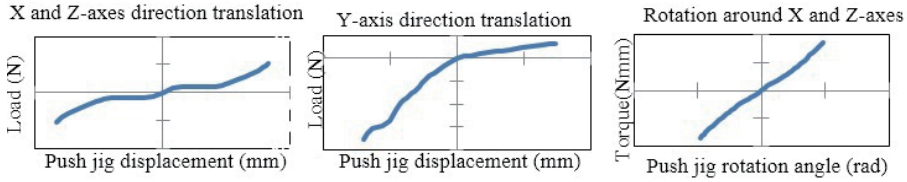

Figure 28: Results of grommet rigidity simulation

12 VERIFICATION OF RADIATOR ASSEMBLY STRENGTH SIMULATION

Figure 29 shows the conditions of total internal energy and total kinetic energy generation. Both of these energy types represent the total energies for all elements of the radiator and plastic cover. The percentage of total kinetic energy relative to total internal energy is on the order of several percent, showing that a valid solution can be provided by addressing the issue as a quasi-static problem.

Figure 30 shows the load-displacement curves from the simulation models and test results. The load and displacement represent the reaction force acting on the push jig in the X-axis direction and the displacement in the X-axis direction. The maximum load is approximately 30% higher in the simulation result than the test result. The generated load was approximately 10% higher than the test result in the plastic cover model, and approximately 20% higher in the radiator model. This 30% deviation is thought to be the combined error resulting from the above.

The conditions of plastic cover buckling and radiator deformation after the load was removed are shown in Figure 31. The buckled part of the plastic cover correlates with the test results. For the radiator, the same damage conditions of overall twisting were reproduced.

Based on the above verification results, it is believed that this radiator assembly strength simulation can be used to predict the test results. The use of this simulation method will allow detailed analysis of radiator and plastic cover behavior during the test which is otherwise difficult to observe from testing alone, and will be effective as a means of identifying locations for strength countermeasures.

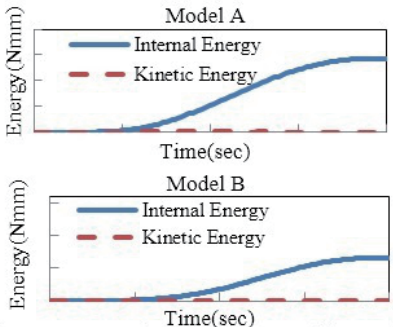

Figure 29: Energy in radiator assembly model

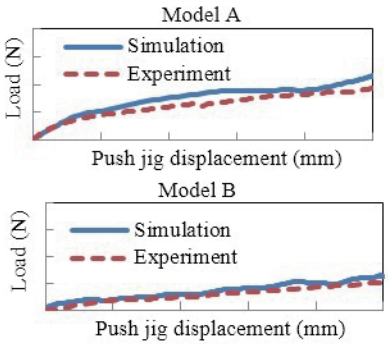

Figure 30: Radiator assembly model load-displacement curves

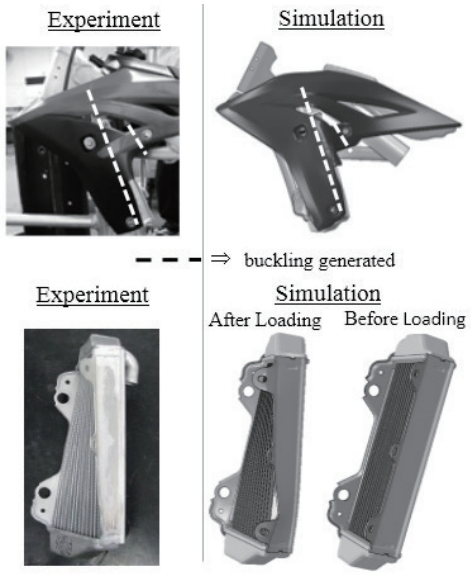

Figure 31: Conditions of radiator assembly deformation

13 CONCLUSION

Strength tests were conducted for the radiator assembly of an off-road motorcycle, and the test results were used to verify the validity of the simulation model. By considering the strain rate sensitivity of the plastic cover, and creating a model of the radiator fins using a user material (dynamic stress-strain relation in Abaqus), good correlation of the simulations with the results of the tests was achieved. Based on the series of verification results, it is believed that the radiator assembly strength simulation can be used to predict the test results, and that this simulation method will be an effective design support tool.

REFERENCES

[1] Hiroyuki Mae ,et al. :"Non-linear, Strain Rate-dependent Behavior of Polymer at Room Temparature: Experimental Findings and Calculation Results", JSAE Paper Number: 20045039 May, 2004 Issued No.45-04

[2] Masahiro Fuji ,et al.: "Benchmark Problem of Crush Analysis of Plastic Parts for Automotives.", JSAE Paper Number: 9940620 Oct, 1999 Issued No.88-99

[3] Masahiro Fuji ,et al.: "Study of Impact Analysis for Plastic Parts with Rib Structure Part I Benchmark Problem of Crush analysis and results of experiment", JSAE Paper Number: 20005158 May, 2000 Issued No.63-00

[4] Norikazu Matsuura ,et al.: "Study of Impact Analysis for Plastic Parts with Rib Structure Part II Influence of Finite Element Modeling on Deformation and Load Response", JSAE Paper Number: 20005089 May, 2000 Issued No.63-00

[5] Kenji Takada ,et al.: "Study of Impact Analysis for Plastic Parts with Rib Structure Part III An Investigation of Material Modeling to Improve the Accuracy of Impact Analysis", JSAE Paper Number: 20005160 May, 2000 Issued No.63-00

[6] Makoto Nagamori ,et al.: "Study of Impact Analysis for Plastic Parts with Rib Structure Part IV The relations of deform phenomena and response force between unit cell and several lattice structure", JSAE Paper Number: 20005233 May, 2000 Issued No.63-00

[7] Abaqus User's Manual

■著者

山谷 真和
Masakazu Yamaya
技術本部
研究開発統括部
基盤技術研究部

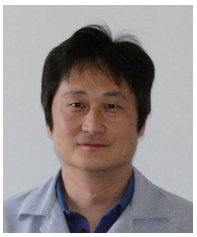

千葉 晃広
Akihiro Chiba
技術本部
研究開発統括部
基盤技術研究部